European Journal of Pharmaceutics and Biopharmaceutics 188 (2023) 137–146

Contents lists available at ScienceDirect

European Journal of Pharmaceutics and Biopharmaceutics

journal homepage: www.elsevier.com/locate/ejpb

Research paper

High energy ball milling vs. nano spray drying in the development of supersaturated systems loaded with bosentan

Anna Krupa [a,b,*], Florence Danède [b], Dorota Majda [c], Agnieszka Węgrzyn [c], Dominik Strojewski [a], Ita Kondera [a], Jean-François Willart [b]

[a] Jagiellonian University, Medical College, Faculty of Pharmacy, Department of Pharmaceutical Technology and Biopharmaceutics, 9 Medyczna Street, 30-688 Cracow, Poland

[b] University of Lille, CNRS, INRAE, Centrale Lille, UMR 8207, UMET – Unité Matériaux et Transformations, F-59000 Lille, France

[c] Jagiellonian University, Faculty of Chemistry, 2 Gronostajowa Street, 30-387 Cracow, Poland

ARTICLE INFO

Keywords:
Bosentan
Supersaturation
Enabling formulations
Solvent evaporation
Mechanical activation
Poorly soluble drugs

ABSTRACT

In this study, high energy ball milling and nano spray drying were used to prepare amorphous solid dispersions of bosentan in copovidone for the first time. In particular, the impact of this polymer on the bosentan amorphization kinetics was investigated. Copovidone was shown to facilitate the amorphization of bosentan upon ball milling. As a result, bosentan was dispersed in copovidone at the molecular level, forming amorphous solid dispersions, regardless of the ratio of the compounds. The similarity between the values of the adjustment parameter that describes the goodness of fit of the Gordon-Taylor equation to the experimental data ($K = 1.16$) and that theoretically calculated for an ideal mixture ($K = 1.13$) supported these findings. The kind of coprocessing method determined the powder microstructure and the release rate. The opportunity to prepare submicrometer-sized spherical particles using nano spray drying was an important advantage of this technology. Both coprocessing methods allowed the formation of long-lasting supersaturated bosentan solutions in the gastric environment with maximum concentrations reached ranging from four (11.20 μg/mL) to more than ten times higher (31.17 μg/mL) than those recorded when the drug was vitrified alone (2.76 μg/mL). Moreover, this supersaturation lasted for a period of time at least twice as long as that of the amorphous bosentan processed without copovidone (15 min vs. 30–60 min). Finally, these binary amorphous solid dispersions were XRD-amorphous for a year of storage under ambient conditions.

1. Introduction

Bosentan (4-(1,1-dimethylethyl)-*N*-[6-(2-hydroxyethoxy)-5-(2-methoxyphenoxy)[2,2′-bipyrimidin]-4-yl] benzenesulfonamide) is a mixed endothelin receptor antagonist approved for the treatment of symptoms associated with pulmonary arterial hypertension and scleroderma. This compound shows high physicochemical stability, as it is not hygroscopic or light sensitive, but is poorly soluble in water (<2 μg/mL), and therefore its bioavailability after oral administration is limited to 50 % [1]. Currently, tablets loaded with the drug dose of 62.5 mg or 125 mg are used in pharmacotherapy. However, bosentan is hepatotoxic and its chronic administration is often related to the increase in aminotransferase level, which is one of the most important reasons for discontinuation of treatment [2,3]. Thus, the enhancement of the drug solubility and in consequence its bioavailability, which could provide the opportunity to reduce the drug dose, is of particular interest.

There are reports that the solubility enhancement was possible after amorphization of bosentan monohydrate by melt quenching, cryomilling [4], high energy ball milling at ambient conditions [5] **or spray drying** [6]. Moreover, its amorphous form was stable and did not recrystallize for at least 6 months [5].

Due to the presence of a functional sulfonamide group in the chemical structure, bosentan shows acidic properties (**pKa = 5.46**). The concentration of the amorphous bosentan dissolved in the gastric milieu was more than twice as high as that of the crude crystalline drug [5] and reached maximum after 10–15 min. However, this concentration–time profile showed a spring pattern typical of metastable supersaturated

* Corresponding author at: Jagiellonian University, Medical College, Faculty of Pharmacy, Department of Pharmaceutical Technology and Biopharmaceutics, 9 Medyczna Street, 30-688 Cracow, Poland.
E-mail address: a.krupa@uj.edu.pl (A. Krupa).

https://doi.org/10.1016/j.ejpb.2023.05.014
Received 20 February 2023; Received in revised form 22 April 2023; Accepted 12 May 2023
Available online 15 May 2023

systems, because amorphous bosentan recrystallized rapidly in contact with simulated gastric fluid (SGF). As a consequence, the concentration of the drug dissolved sharply decreased to reach the equilibrium in<30 min. Due to the fact that SGF does not contain surfactants, floating particles were visible on the surface of the solvent until the end of the study (120 min). These findings provide evidence that a sole amorphization of bosentan can be insufficient to effectively enhance its performance *in vivo* and that the combination of this poorly soluble drug with wetting agents or surfactants, e.g. hydrophilic polymers, seems necessary.

In this context, Panda et al. [7] proposed the fabrication of lipid-based formulations, using a self-emulsifying surfactant, i.e. macrogol-32 stearoyl glycerides (Gelucire 50/13, HLB = 11; CMC = 100 mg/L). They were melted together with a poly(ethylene glycol)-*block*-poly(propylene glycol)-*block*-poly(ethylene glycol) copolymer (poloxamer 188). As a consequence, a significant increase in drug solubility was possible, which was 8 to 10 times greater than that of crude bosentan. Kendre and Chauhari [8] developed bosentan nanocomposites in an amphiphilic graft copolymer composed of polyvinyl caprolactam – polyvinyl acetate - polyethylene glycol (Soluplus) in a single emulsification technique. They concluded that the amorphization of the drug together with its encapsulation within the polymer matrix allowed its solubility to be enhanced more than five times in comparison to that recorded for physical mixtures or unprocessed bosentan. Finally, this gain in solubility resulted in the bioavailability enhancement shown in a rabbit model. On the basis of these promising results, the authors proposed buccoadhesive tablets loaded with solid dispersions of bosentan in Soluplus [9].

In the present study, copovidone (Kollidon VA64) was chosen, for the first time, as a carrier to form solid dispersions loaded with bosentan. This polymer has highly hydrophilic properties and can be used as a wetting agent for hydrophobic drug particles. It could, therefore; create long-lived supersaturated solutions of poorly soluble bosentan in the gastrointestinal tract with a beneficial impact on its absorption [10]. An important advantage of copovidone is also its relatively high glass transition temperature ($Tg = 106\,^{\circ}C$). This value is much higher than that of bosentan amorphous, that is, **50 °C and 82 °C for amorphous bosentan monohydrate and anhydrous, respectively** [5]**. Thus, copovidone should also effectively prevent the recrystallization of amorphous drug after storage under ambient conditions.**

The aim of this study was to prepare homogeneous amorphous solid dispersions in which bosentan was **dispersed at the molecular level in copovidone. Two fundamentally different co-amorphization methods, namely high energy ball milling and nano spray drying, were used to produce the amorphous solid dispersions, and their impact on the physical properties and dissolution of bosentan was compared. The choice of the high energy ball milling technique was dictated by previous experiments, which have demonstrated that this method could be applied to produce successfully and rapidly amorphous bosentan** [5]**. Interestingly, this solid state amorphization does not require the heating of ingredients or the use of organic solvents, which reduces the risk of thermal decomposition of the drug and the toxicity of the formulation. Moreover, nano spray drying** is **preferred to conventional spray drying as it gives the opportunity to prepare amorphous solid dispersions of submicrometer particle size and a narrow particle size distribution, even if only a small amount of the sample is available.** This approach is of particular interest in the early stages of drug development when there is only a limited amount of the compound or if expensive or labile drugs are to be processed. When considering the fact that the price of bosentan is relatively high, ca. 10 000 USD/kg, the application of nano spray drying to form amorphous solid dispersions can be an interesting option for the laboratory-scale development of enabling sub-micrometer formulations loaded with this drug. For technical details on nano spray drying, an interested reader is encouraged to refer to the latest articles by Almansour et al. [11], Arpagaus [12,13]; Arpagaus et al. [14]. The most important advantages of nano spray drying rely on gentle processing conditions and a high-yield collection of submicron particles [11,15,16]. As a result, many examples of crystalline or amorphous submicrometer particles loaded with metronidazole [17], sildenafil [18], or naproxen [19] have been developed using this technology.

In this research, our attention was focused on the physical properties and drug release from amorphous solid dispersions prepared using co-milling and nano spray drying. Evaluation of their physical properties was carried out with the aim to assess both homogeneity and stability of these coamorphous samples. For this purpose, powder X-ray diffraction (XRD) and differential scanning calorimetry (DSC) were applied. These two main techniques were combined with spectroscopic methods (ATR, ^{1}H NMR) and scanning electron microscopy (SEM). **Finally, drug release studies were performed under non-sink conditions using two different media, that is, simulated gastric fluid of pH = 1.20 and phosphate buffer of pH = 6.80 to simulate *in vitro* the environment of the gastrointestinal tract (GIT).**

2. Materials and methods

Samples of bosentan monohydrate (BOS) and copovidone (VA, Kollidon VA64) were kindly donated by Polpharma S.A. (Starogard Gdański, Poland) and BASF Poland (Warsaw, Poland) respectively.

Analytical grade dimethyl chloride was purchased from Chempur (Piekary Śląskie, Poland). 36 % hydrochloric acid was obtained from Merck (Warsaw, Poland). Natrium chloride, potassium dihydrogen phosphate, and disodium hydrogen phosphate were purchased from Avantor Performance Materials Poland S.A. (Gliwice, Poland). All of these reagents were of analytical grade.

The 50 % acetic acid for HPLC was supplied by Sigma-Aldrich Co. (St. Luis, MO, USA). Acetonitrile for HPLC of isocratic grade was purchased from Witko (Łodź, Poland). Purified water was prepared household using a Milli-Q Elix Essential water purification system of Millipore Corporation (Merck, Warsaw, Poland). **Dimethyl sulfoxide (DMSO) was purchased from Carl Roth GmbH (Karlsruhe, Germany), whereas DMSO-d_6 and deuterated chloroform ($CDCl_3$) were obtained from Deutero GmbH (Kastellaun, Germany).**

2.1. Preparation of solid dispersions

2.1.1. Milling protocol

High energy ball milling (BM) was carried out at room temperature (RT) using a Pulverisette 7, Fritsch (Idar-Oberstein, Germany) planetary ball mill. Binary mixtures (1.1 g) composed of bosentan monohydrate and copovidone were placed in 45 mL milling jars with seven milling balls of 15 mm in diameter. The weight fraction of bosentan (X_{BOS}) in these mixtures varied from 0 to 1. **The polymer load was investigated at three levels which corresponded to the following weight fractions 0.2; 0.5 and 0.8. The sample name was, therefore; composed of the abbreviation of the coprocessing method (BM) followed by the bosentan fraction, i.e. BM0.2 was composed to 20 wt% of bosentan and 80 wt% of copovidone. These binary formulations were placed in the milling jars made of zirconium oxide together with seven milling balls (Ø = 15 mm) of the same material, which led to a ball-to-sample weight ratio of 75:1**. The rotational speed of the solar disc was set at 400 rpm. The milling was performed for 5 min, 10 min, 20 min, 60 min, 120 min, 240 min and 360 min. For milling periods longer than 20 min, the milling time of 20 min was alternated with 10 min pause periods to avoid overheating of the samples.

For comparison, bosentan monohydrate was also milled alone (240 min). Binary physical mixtures (PM) composed of crystalline bosentan and copovidone were prepared together with physical mixtures in which amorphous ball-milled bosentan (240 min) **was manually blended**

with the polymer until a homogeneous mixture was formed (ca. 5 min).

2.1.2. Nano spray drying

This coprocessing was performed using a nano spray dryer (B-90 Advanced, Büchi Labortechnik, Flavil, Switzerland) in a short setup, i.e. 110 cm in height, and a closed-loop configuration where the main unit was coupled with an inert loop (B 295 SE, Büchi Labortechnik, Flavil, Switzerland) for an organic solvent recovery and a dehumidifier (B 296, Büchi Labortechnik, Flavil, Switzerland). Nitrogen was used as a drying gas.

First, bosentan monohydrate and copovidone were dissolved in dichloromethane (DCM). The bosentan concentration was kept at 1 % *(w/w)* and the copovidone load was adjusted to form polymeric solutions in which the drug weight fraction (X_{BOS}) ranged from 0.20 to 0.80 respectively (Table 1). Upon co-processing, these solutions were ice cooled and recirculated over a spray mesh of size M using a peristaltic pump. The spray intensity was set at 70 %, the spray frequency was 120 kHz and the gas flow rate ranged between 110 and 120 L/min. The inlet temperature was set at 55 °C, resulting in the outlet temperature of 38 °C. The nano spray-dried samples were placed in glass vials and also dried at 60 °C for 8 h in a laboratory oven (FD-S 115, Binder GmbH, Tuttlingen, Germany). Then the vials were tightly closed and stored in a desiccator on a silica gel at ambient conditions.

2.2. Particle morphology

The powder samples were adhered to a holder with double-sided copper tape. Their surface was coated with carbon using a 208 HR carbon sputter coater (Cressington Scientific Instruments, Watford, UK). Then, their morphology was analyzed by a Hitachi S-4700 (Japan) scanning electron microscope (SEM). The images were taken at a magnification of 100 ×, 2 000 × and 20 000 x. ImageJ v.1.53a software (NIH, USA) was used to estimate the particle size.

2.3. Powder X-ray diffraction (XRD)

2.3.1. High energy ball milled formulations

The experiments on co-milled samples were carried out with a PanAlytical X'Pert PRO MPD diffractometer (Almelo, The Netherlands), equipped with X'Celerator detector. For measurements carried out in RT, the samples were placed in Lindemann glass capillaries 0.7 mm in diameter (Hilgenberg GmbH, Masfeld, Germany). The capillaries were installed on a rotating sample holder to avoid any artifacts due to preferential orientations of crystallites. All samples were exposed to X-ray radiation (λCu − Kα) with a wavelength of 1.540 Å. The diffractograms were recorded from 5 to 40° or 60°, with a scan step of 0.0167°/sec.

Table 1
The composition of nano spray dried formulations and corresponding process conditions.

Nano spray drying (NSD)		NSD0.8	NSD0.5	NSD0.2
Formulations variables	Bosentan load in DCM [%, *w/w*]	1	1	1
	Copovidone load in DCM [%, *w/w*]	0.25	1	4
	Total solid load in DCM [%, *w/w*]	1.25	2	5
Process parameters	Inlet temp. [°C]	55		
	Outlet temp. [°C]	38		
	Nebulizer mesh size [μm]	5.5		
	Spray frequency [kHz]	120		
	Spray intensity [%]	70		
	Gas flow rate [L/min]	110–120		

2.3.2. Nano spray dried formulations

The nano spray dried samples, placed in disc holders, were tested using a powder X-ray diffractometer (Bruker, D2 Phaser, Billerica, MA, USA) equipped with CuKα radiation source (λ = 0.154184 nm; measurement range 2-70° 2θ; step size 0.02° 2θ; slit width 0.6 mm; step scan size 0.02°; counting time 1 s; voltage 30 kV, current 10 mA).

2.4. Differential scanning calorimetry (DSC)

2.4.1. High energy ball milled formulations

A differential scanning calorimeter DSC Q1000 (TA Instruments, Guyancourt, France) equipped with a refrigerated cooling system was used to characterize the solid-state properties of bosentan. The temperature and enthalpy readings were calibrated using pure indium at the same scan rates as those used in all the experiments. Samples (3–5 mg) were placed in open aluminium pans (container without lid) to facilitate the evaporation of water. During the measurement, the calorimeter head was purged with highly pure nitrogen gas (50 mL/min). **Prior to the measurements the samples were heated at 60 °C for at least 15 min to evaporate water**. The scans were performed at 5 °C/min from 20 °C to 130 °C (the first heating scan). The samples were then cooled to 20 °C and the second heating scan was performed to 130 °C (5 °C/min).

2.4.2. Nano spray dried formulations

Measurements were carried out using a Mettler Toledo DSC 3 + differential scanning calorimeter (Switzerland) with the software STARe v.16.4. The sample (ca. 5 mg) was placed in an aluminium pan sealed with a pierced lid. It was heated to 60° C and stabilized at this temperature for 30 min. After this isothermal program, the sample was cooled from 60 °C to 20 °C. The cooling rate was 5 °C/min. The sample was then heated from 20 °C to 130 °C with the heating rate of 5 °C/min (the first heating scan). Then it was cooled down from 130 °C to 20 °C and again heated from 20 °C to 130 °C (the second heating scan). The measurements were carried out in an Ar atmosphere with gas flow of 50 mL/min.

2.5. Drug release studies

The release of bosentan from solid dispersions was studied in non-sink conditions using two different media, i.e. simulated gastric fluid (SGF, Ph. Eur. 10th Ed., pH = 1.20) without pepsin or phosphate buffer of pH = 6.80 (PBS). The tests were carried out at 37 °C ± 0.5° C. An automated pharmacopoeial paddle dissolution apparatus, Hanson Research Dissolution Station Vision Elite 8 with an autosampler Visione AutoPlus™ Maximizer and a sample collector AutoFill™ device (Chatsworth, CA, USA) equipped in a set of small vessels (150 mL) was used. Each test was carried out with samples corresponding to 20 mg of bosentan and 100 mL of SGF or PBS. The paddle rotation speed was set at 75 rpm. Samples of 2 mL were withdrawn for 120 min and the same amount of replacement medium was added. The samples were transferred to test tubes containing acetonitrile (0.2 mL – 2 mL). Then, they were vortexed and filtered directly into HPLC vials. The concentration of bosentan dissolved was determined using the HPLC method described below. The mean values (n = 3) in μg mL^{-1} and the corresponding standard deviations were calculated.

2.6. HPLC-DAD method

The concentration of dissolved bosentan was determined using an Agilent 1260 Infinity HPLC system (Waldbronn, Germany) connected to a diode array detector (DAD). **The samples of 2 mL** were filtered through a nylon syringe filter (Ø = 0.45 μm). They were analyzed using an InfinityLab Poroshell 120EC-C18 (4.6 × 100 mm; particle size 4 μm) reversed phase LC column with the corresponding guard column. The injection volume was 5 μL. The mobile phase was composed of acetonitrile (ACN) and 0.1 % *(v/v)* acetic acid mixed in a 60:40 *(v/v)* ratio

(isocratic elution). The flow rate was 0.8 mL min^{-1}. The column oven temperature was set at 25 °C. The bosentan signal was detected at a wavelength of 267 nm. **A mixture of ACN and DMSO (9 + 1) was used as a needle wash solvent.**

The calibration curve was prepared using crude bosentan monohydrate as a standard to prepare a stock solution of 1 mg mL^{-1} in ACN. The composition of a dilution solvent reflected conditions of drug release studies performed using either in SGF or PBS, including addition of ACN (0.2 mL − 2 mL) to prevent drug precipitation. The calibration curve was linear within the following ranges: 3.2–36.0 μg mL^{-1} (r^2 = 0.9997) for SGF with LOD = 0.97 μg mL^{-1} and LOQ = 2.93 μg mL^{-1}, and 2.0–100.0 μg mL^{-1}(r^2 = 0.9998) for PBS with LOD = 0.77 μg mL^{-1} and LOQ = 2.33 μg mL^{-1}.

3. Results and discussion

3.1. Impact of high energy ball milling on crystallinity of bosentan coprocessed with copovidone

Fig. 1a shows diffractograms recorded at RT immediately after co-milling of bosentan with copovidone **(1:1)** for a period of time ranging from 5 min to 360 min. For the sake of comparison, the diffraction patterns of crude bosentan monohydrate and copovidone are presented as well. The broadening of sharp X-ray peaks typical of crystalline bosentan monohydrate, together with a gradual decrease in their intensity, is visible during the co-milling process. It was observed that after 120 min of milling, the sharp peaks became invisible. There was only a *halo* pattern, indicating a full amorphization of bosentan.

The heat flow curves (5 °C/min) of the binary co-milled formulation recorded after increasing milling times are presented in Fig. 1b and compared to those of crude compounds. Before recording, all samples were heated at 60 °C for 15 min in the DSC apparatus with the aim of removing the water from bosentan monohydrate that could mask and depress the glass transition. As previously reported [5], the DSC scan of crude anhydrous bosentan showed a melting endotherm at 112 °C. The analysis of quenched bosentan revealed that its glass transition temperature (Tg = 82 °C) was close to the melting point. Importantly, crude bosentan was found to be a very good glass former with high stability against recrystallization [5]. **The comparison of the heat flow curves (5 °C/min) recorded for the samples loaded with bosentan and copovidone (1:1) indicates that the bosentan melting peak slightly shifted towards the low temperatures and strongly decreased during the first 20 min of milling.** This indicates a progressive and rapid amorphization of bosentan during milling. After 120 min of milling, the melting peak has totally disappeared, and a clear underlying Cp jump characteristic of a glass transition was clearly seen. This glass transition (Tg = 95 °C, ΔCp = 0.39 J/g·°C) was located between those of the pure compounds that could no longer be detected. Thus, co-milling led to a homogeneous amorphous solid dispersion of bosentan into PVP VA64. No further evolution of the thermogram could be observed for a longer milling time (up to 360 min), indicating that a stationary state was reached. Note that **several thermal events occur in a narrow temperature range: the glass transition of pure copovidone, that of pure bosentan and that of the final solid dispersion, as well as the melting of crystalline bosentan. This results in a partial overlapping of the corresponding thermal events which makes difficult to judge from the homogeneity of the dispersion during the first minutes of milling where all components coexist**. However, some traces of the glass transition of pure bosentan could be detected on the left wing of the melting **peak** during the first 20 min of milling, suggesting that pure amorphous bosentan was produced before it came to enrich the amorphous solid dispersion.

Importantly, there was no recrystallization of the amorphous drug after heating the semi-crystalline or fully amorphous binary formulations to 130 °C. The same thermal behavior, i.e. the ease of amorphization together with an unexpectedly high stability of the amorphous form while heating, had been described for bosentan monohydrate high energy ball milled alone [5].

The amorphization kinetics of bosentan in the presence of copovidone was analyzed as well. Fig. 2 shows a good fitting of the exponential relaxation law Eq. (1) to the experimental data showing the evolution of the amorphous bosentan fraction as a function of the milling time.

$$X_{am}(t) = 1 - \exp(t/\tau) \quad (1)$$

The amorphous fraction (X_{am}) was calculated according to Eq. (2), where ΔH_m is the enthalpy of melting of non-milled anhydrous bosentan and ΔH_m^{milled} is the enthalpy of melting of crystalline bosentan in ball milled samples.

$$X_{am} = 1 - \left(\Delta H_m^{milled}/\Delta H_m\right) \quad (2)$$

It was revealed that bosentan could be amorphized very rapidly upon

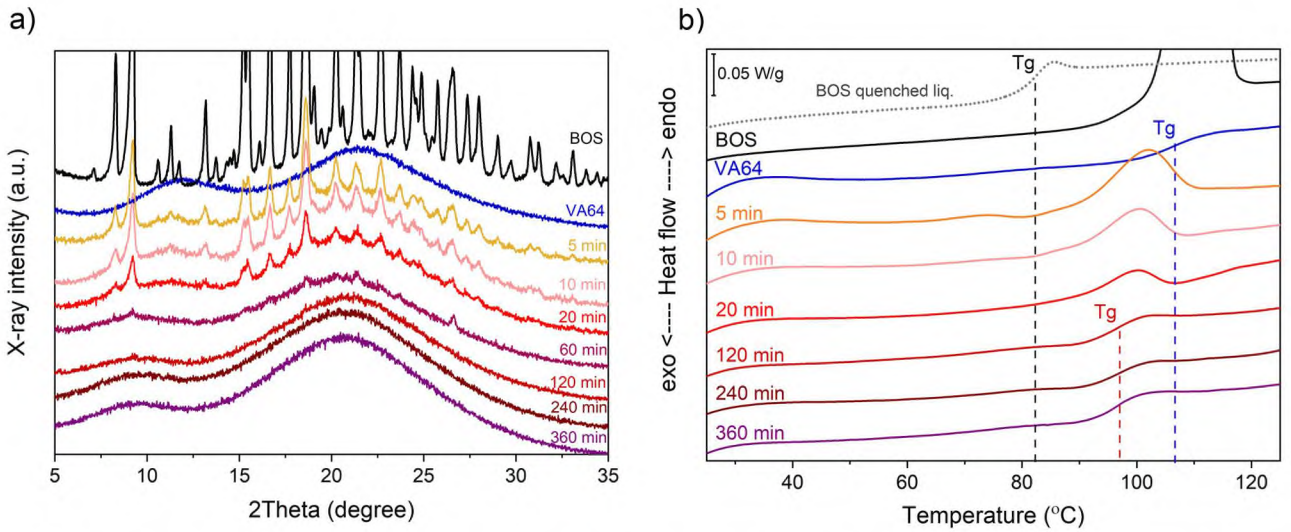

Fig. 1. Impact of milling time **(shown as labels in min)** on powder X-ray diffraction patterns (a) and heating (5 °C/min) DSC scans (b) of bosentan monohydrate comilled with copovidone (1:1). XRD patterns were recorded just after milling. The DSC scans were recorded after 15 min annealing at 60 °C to remove water from the sample. XRD patterns of Kollidon VA64 and bosentan **monohydrate** were added for comparison. Heating DSC scans of Kollidon VA64, **bosentan anhydrous, and melt quenched bosentan monohydrate were also provided**.

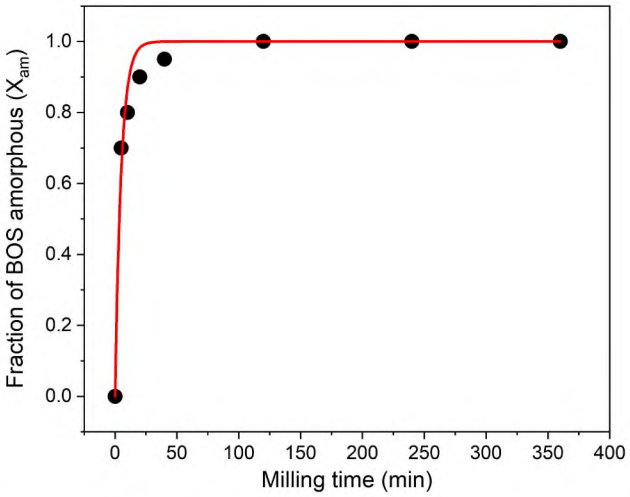

Fig. 2. Amorphization kinetics of bosentan monohydrate upon comilling with copovidone **(1:1)**. Fitting of the experimental curve by the exponential relaxation law given by Eq. (1) is shown as a solid red line ($r^2 = 0.978$). (For interpretation of the references to colour in this figure legend, the reader is referred to the web version of this article.)

milling alone. Its relaxation time was more than ten times shorter than that recorded for other active pharmaceutical ingredients considered good glass formers such as dexamethasone [20], chlorhexidine [21] or lactulose [22], amorphized using the same procedure. The relaxation time derived from the fit ($\tau = 5.0$ min) appears to be slightly shorter than that determined for pure bosentan ($\tau = 6.6$ min [5]), indicating that the presence of copovidone facilitates the amorphization of the drug.

The impact of the copovidone load (20, 50 or 80 wt%) on the crystallinity of bosentan after comilling for 240 min is shown in Fig. 3. The absence of Bragg peaks in the XRD patterns revealed a complete amorphization of bosentan upon comilling with copovidone, regardless of the drug-to-polymer ratio. The DSC scans of the three studied co-milled mixtures are presented in Fig. 4. All exhibited a single glass transition whose **mid-inflection point** shifted to higher temperatures (87–102 °C) as the polymer load in the sample increased (20–80 %), indicating its antiplasticizing effect. **These results indicated that bosentan formed amorphous solid dispersions in copovidone regardless of the drug to the polymer ratio.** Thus, the amorphous

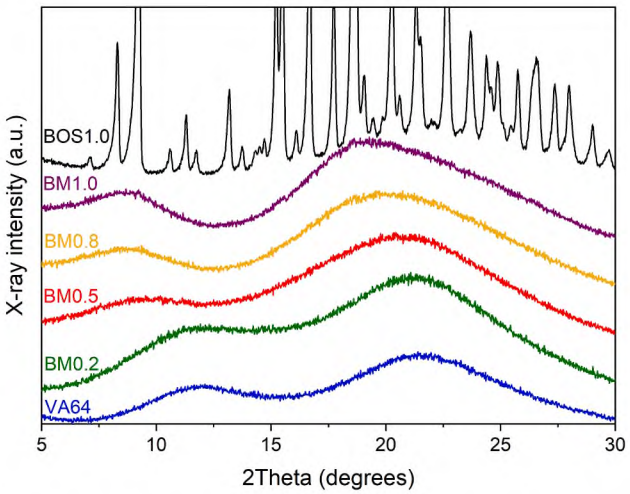

Fig. 3. XRD patterns of BOS **monohydrate** / copovidone physical mixtures co-milled for 240 min. The drug **fraction** ranged from 0 to 1 as indicated on the left-hand side of each curve. BOS1.0 stands for unmilled bosentan **monohydrate**.

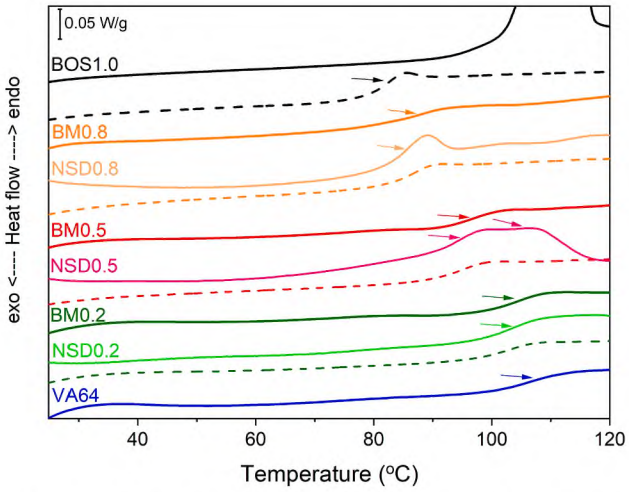

Fig. 4. Heating (5 °C/min) DSC scans of physical BOS monohydrate / copovidone mixtures co-milled for 240 min (BM) in comparison to nano spray dried samples (NSD). Bosentan fraction ranged from 0 to 1 as indicated in abbreviated sample name. BOS1.0 stands for unmilled bosentan anhydrous, whereas VA64 stands for crude copovidone. Solid lines represent first heating scans, dash lines show second heating scans. All DSC scans were recorded after at least 15 min of annealing at 60 °C to remove water from studied samples.

formulations rich in bosentan (e.g. BM0.8 **where wt. fraction of bosentan = 0.8**) could be prepared under ambient conditions. Furthermore, a mechanical activation of these molecules gives the opportunity to manufacture stable glassy solutions without the need for either a thermal treatment or organic solvents.

To evaluate the strength of interactions between bosentan and copovidone in their binary glassy solutions and then to be able to calculate the *Tg* for any component ratio, the experimental data *(Tg)* recorded for representative binary formulations and those of single compounds were plotted in Fig. 5. Then, these data were fitted by the Gordon-Taylor equation **Eq. (3)**:

$$Tg(X_{BOS}) = \left[X_{BOS} \cdot Tg^{BOS} + K \cdot (1 - X_{BOS}) \cdot Tg^{VA64}\right] / \left[X_{BOS} + K \cdot (1 - X_{BOS})\right] \quad (3)$$

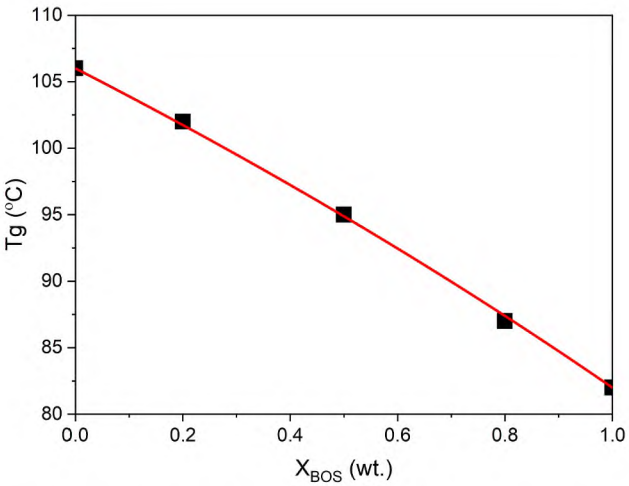

Fig. 5. Gordon-Taylor (GT) plot showing variations of Tg in bosentan-copovidone amorphous solid dispersions obtained by a 240 min high energy ball milling of the crystal. The fitting of the experimental curve by the GT equation is shown as a solid red line ($r^2 = 0.999$). (For interpretation of the references to colour in this figure legend, the reader is referred to the web version of this article.)

where X_{BOS} is a weight fraction of bosentan in the formulation, Tg^{BOS} and Tg^{VA64} are, respectively, the glass transition temperatures of crude bosentan and copovidone, and K is a fitting parameter, describing the curvature of the evolution. The best fit was obtained for $K = 1.16 \pm 0.03$, which is very close to the K_{id} value expected for an ideal mixture **Eq. (4)**:

$$K_{id} = \Delta C_p^{VA64} / \Delta C_p^{BOS} = 0.53\ (J/g\cdot{}^{\circ}C) \,/\, 0.47\ (J/g\cdot{}^{\circ}C) = 1.13 \qquad (4)$$

where ΔCp_{VA64} and ΔCp_{BOS} are the amplitude of heat capacity *(Cp)* jump at *Tg* of copovidone and bosentan, respectively.

The ATR-IR and ^{1}H NMR spectra recorded in DMSO-d_6 or $CDCl_3$ (see Appendix Fig. A.2-A.4) confirmed that, apart from the features typical of amorphous systems, there were no signs of strong interactions between the components nor chemical degradation of the solid dispersion components engendered by coprocessing. Importantly, when they were tested after one year of storage in RT, their chemical properties remained unchanged.

The physical stability of a glassy solution depends on the miscibility of the compounds and the Tg of the final formulation. As a general rule, if its *Tg* is more than 50 °C higher than the storage temperature (*T*), the mobility of the molecules is weak and the risk of recrystallization in dry conditions is low [23]. Given this assumption, the impact of copovidone load on glassy solution stability was theoretically evaluated at three common drug storage temperatures, that is, 0 °C, 25 °C and 40 °C. The calculated differences between *Tg* and *T* are shown in Table 2. They confirm the suitability of copovidone to **potentially** protect amorphous bosentan from recrystallization even if only 20 wt% of the polymer was used. However, **in theory**, to ensure the stability of the glassy solution at 40 °C, the polymer load should preferably be higher than 50 wt%.

3.2. Impact of nano spray drying on the crystallinity of bosentan coprocessed with copovidone

Fig. 6 shows XRD patterns recorded for nano spray dried solid dispersion of bosentan loaded with 50 wt% of copovidone immediately after preparation and after a year of storage under ambient conditions. Regardless of the polymer load, the Bragg peaks of crystalline bosentan disappeared after such a processing, indicating the amorphization of bosentan or formation of nanocrystals. The same was true for spray dried solid dispersions loaded with 20 or 80 wt% of the drug **(**Fig. A.5**)**. Similarly to high-energy ball milled amorphous solid dispersions, nano spray dried formulations remained also XRD-amorphous, after a year of shelf life (Fig. 6).

To verify the structural state of spray dried solid dispersions, DSC heating scans were recorded using a heating–cooling-reheating protocol similar to that applied for the analyses of high energy ball milled solid dispersions. The first heating scans recorded after 30 min of heating of the samples at 60 °C to remove water are shown in Fig. 4. In contrast to high energy ball milled samples, the DSC scans of nano spray dried systems loaded with 50 % or 80 % of bosentan showed two glass transitions *(Tg)* revealing some inhomogeneity of the material. The first *Tg* (clearly visible) was lower than that typical of high energy ball milled solid dispersions and corresponded to a fraction **of the amorphous dispersion rich in bosentan**, whereas the second *Tg* (less visible) was related to a fraction rich in copovidone. Thus, the Gordon-Taylor diagram (Fig. 5) was used to estimate the composition of these two amorphous fractions. In the nano spray dried solid dispersion NSD0.8 **(bosentan wt. fraction = 0.8,** Tab. 1**)**, the first *Tg* (mid-inflection point) was at 84 °C, while the second *Tg* was at 98 °C, indicating that the bosentan-rich fraction was loaded with 93 % of the drug and the fraction rich in copovidone was loaded with about 37 % of bosentan. In turn, the first *Tg* in NSD0.5 **(bosentan wt. fraction = 0.5,** Tab. 1**)** was shifted to the higher temperature, that is, 95 °C, indicating a fraction loaded with 50 % of the drug, while the second *Tg* at 104 °C, indicates the presence of a copovidone-rich fraction (<8 % of bosentan). The most homogeneous molecular alloys were formed when 20 % of bosentan was nano spray dried with 80 % copovidone (NSD0.2). In such a case, there was only one *Tg*, located at a position similar to that typical of high energy ball milled counterpart. In general, poorly soluble drugs dissolve in polymers and stable solid solutions are formed if the polymer load is about 70 wt% [24]. Interestingly, the analysis of the second heating scans provides the evidence that quenching of nano spray dried formulations resulted in creating homogeneous systems where only one amorphous glass transition could be seen in DSC heat flow curves, similarly as it had been described for high energy ball milled solid dispersions (Fig. 4).

Table 2
The impact of the copovidone load on Tg and thus on the efficacy to prevent recrystallization of bosentan glassy solutions after storage in dry conditions at the temperature (°C).

Formulation name	Tg (°C)	Tg-T (°C)		
		at 0 °C	at 25 °C	at 40 °C
BM1.0	82	82	57	42
BM0.8	87	87	62	47
BM0.5	95	95	70	55
BM0.2	102	102	77	62

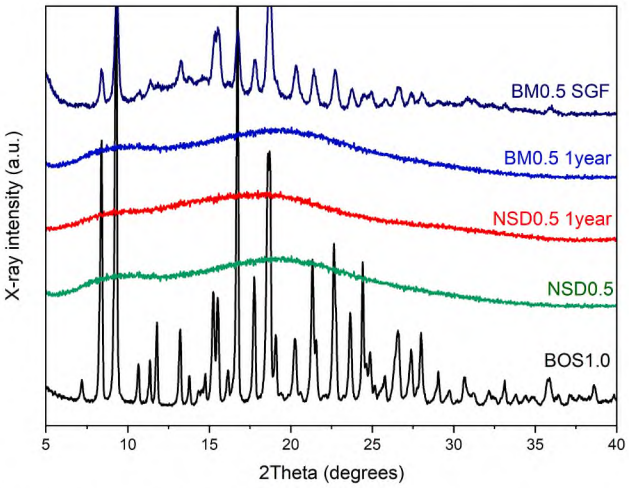

Fig. 6. Diffractograms of high energy ball milled **(BM0.5)** and nano spray dried **(NSD0.5)** solid dispersions of bosentan in copovidone (1:1) recorded after preparation and after a year of storage under ambient conditions compared to **crude bosentan monohydrate** (BOS1.0) and the dried precipitate collected after dissolution studies in SGF (BM0.5 SGF).

3.3. Impact of the manufacturing method on the morphology of solid dispersion particles

Scanning electron micrographs of high energy ball milled and nano spray dried solid dispersions are shown in Figs. 7 and 8 respectively. In particular, the impact of the milling time on the morphology of the solid dispersion is presented in Fig. 7, **whereas the particles size distribution curves determined on the basis of these images are presented in** Fig. A.6**.** The large fragments of agglomerated compounds prevailed in the micrographs of the formulations milled shortly (10 min, Fig. 7 a). Then, according to expectations, their particle size was gradually reduced from 115 μm to ca. 23 μm with increasing milling time (Fig. 7 d-f). However, these fine primary particles of irregular shape had a tendency to form agglomerates of 40–100 μm, which resulted in bimodal or even multimodal particle size distribution (Fig. A.6).

The particles of nano spray dried solid dispersions were about ten times smaller (<2 μm) than those of ball milled samples and, in contrast to them, they were perfectly spherical with only a few irregular particles in the field of view (Fig. 8 a-c). If the polymer load was below 50 wt%,

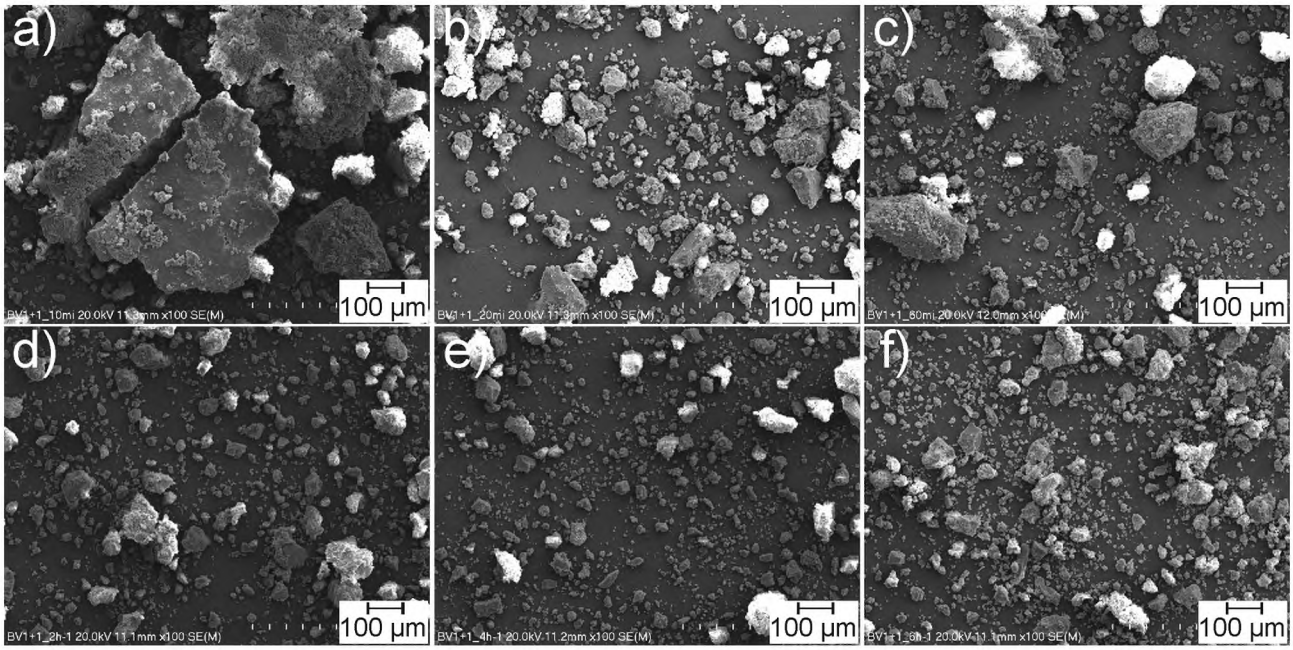

Fig. 7. Impact of increasing milling time on the morphology of solid dispersions composed of bosentan and copovidone coprocessed in 1:1 wt ratio: (a) 10 min, (b) 20 min, (c) 60 min, (d) 120 min, (e) 240 min, (f) 360 min.

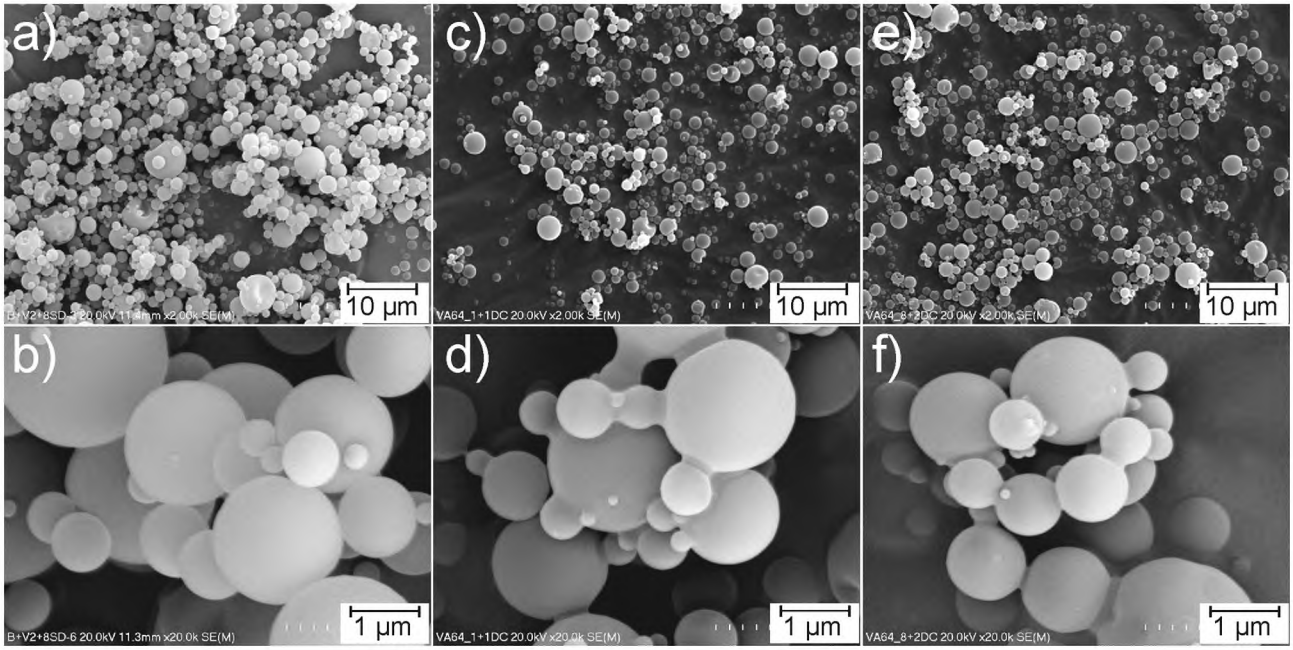

Fig. 8. Impact of decreasing polymer load on the morphology of nano spray dried solid dispersions composed of bosentan and copovidone: NSD0.2 (a, b), NSD0.5 (c, d), and NSD0.8 (e, f).

the big spheres of ca. 1.7 µm were joined by solid bridges with small spheres of 0.6 µm in diameter (Fig. 8 d, f). Furthermore, a fraction of tiny spheres of around 0.2 µm was dispersed on the surface of these branched aggregates.

3.4. *Release of bosentan from solid dispersions in copovidone*

3.4.1. *Impact of milling time on bosentan release from solid dispersions loaded with 50% by weight of copovidone*

In terms of the high energy ball milled formulation loaded with 50 wt % of copovidone, the relationship between the milling time and the shape of the bosentan concentration–time profiles recorded in either SGF or PBS was presented in Fig. 9 a and 9b respectively.

The concentration–time profiles determined in SGF were presented in Fig. 9 a. When the milling time of 240 min or 360 min was applied, the highest concentration of bosentan released was stated with a maximum of 27.23 ± 2.82 µg/mL or 27.54 ± 2.38 µg/mL reached after 30 min. However, a gradual decrease in the concentration of released bosentan was observed after 45 min, and only between 10 and 13 µg/mL of the drug remained dissolved after 120 min. This effect was related to the precipitation of the recrystallizing drug (Fig. 9 a). Different performance was typical of solid dispersions high energy ball milled for 120

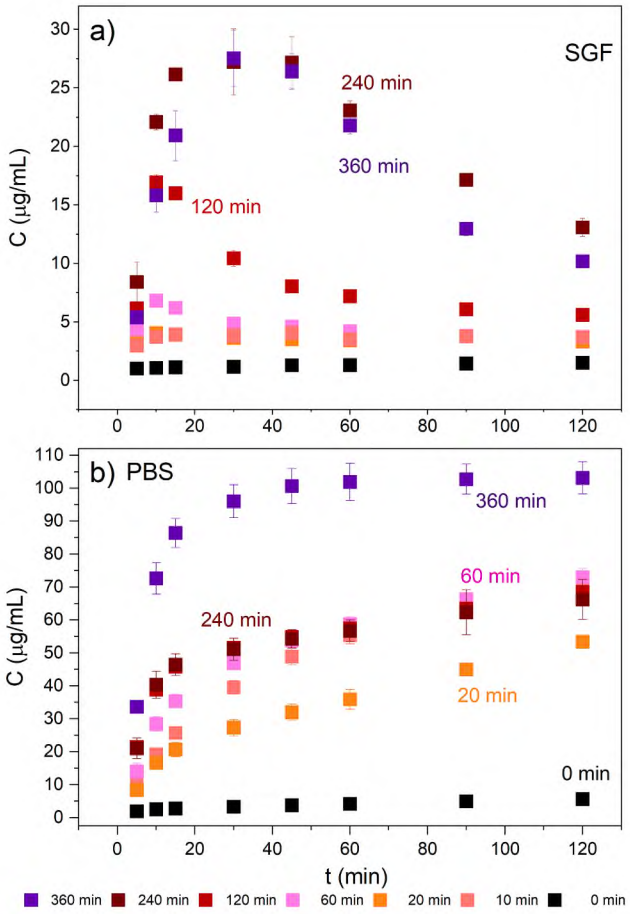

Fig. 9. Impact of milling time on the release of bosentan from solid dispersions in copovidone (1:1): (a) SGF and (b) PBS of pH = 6.80 at 37 °C compared to the binary physical mixture (PM0.5–0 min).

min or 60 min. They showed rapid release of bosentan after 5 or 10 min of study, followed by a sudden drop in its concentration. This effect was particularly pronounced for the solid dispersion ball milled for 120 min, where the maximal concentration **(**Tab. A.2**)** was more than two times higher (16.93 ± 0.66 μg/mL) than that of the formulation processed for 60 min (6.81 ± 0.46 μg/mL). Ball milled formulations for short periods of time, such as 10 or 20 min, showed better performance **(ca. 4 μg/mL)** than that stated for the physical mixture (1.51 ± 0.15 μg/mL). However, their supersaturation levels **(ca. 4 μg/mL)** were more than six times lower than those of the best performing solid dispersions milled for 240 or 360 min, **which were around 30 μg/mL (**Tab. A.2**)**.

Therefore, it can be concluded that the application of copovidone enables supersaturated solutions of bosentan to be obtained in the gastric milieu. However, a full amorphization of bosentan combined with the formation of molecular alloys in copovidone was necessary to create and stabilize supersaturation for the period of time long enough to enhance absorption of bosentan, i.e. at least 30 min. If the traces of crystalline bosentan were present in the sample, they accelerated the recrystallization of bosentan already dissolved in SGF and, finally, its concentration decreased **(**Fig. 9 **a,** Tab. A.2**)**. In our previous study [5], it was found that when fully amorphous, i.e. bosentan milled for 240 min or melt quenched bosentan glass was dissolved in SGF, the maximum concentration was reached after 15 min and was 2.06 ± 0.29 μg/mL or 4.60 ± 0.68 μg/mL respectively. Furthermore, in both cases a sharp decrease in this concentration was also observed up to the saturation level (i.e. < 2 μg/mL).

The concentration–time profiles determined in PBS of pH = 6.80 are presented in Fig. 9 **b**. Since bosentan solubility is pH-dependent (pKa = 5.46) and as its ionization increases with the increasing pH [25], the precipitation of the drug dissolved was not visible regardless of the coprocessing time **(**Tab. A.2**)**. However, when comparing the concentration of bosentan dissolved after 30 min, it was stated that at this time the concentration of bosentan released from the solid dispersion milled for 360 min was much higher (96.02 ± 5.03 μg/mL) than that of the solid dispersion processed for 240 min (51.10 ± 3.31 μg/mL). Additionally, the latter profile was similar to that recorded for the milled for 60 min formulation where 46.92 ± 2.06 μg/mL of bosentan was released. However, mechanical activation of these binary formulations resulted in much higher concentrations of the drug released (regardless of processing time) as compared to the physical mixture of crystalline bosentan with copovidone when only 3.32 ± 0.23 μg/mL or 5.60 ± 0.37 μg/mL of bosentan was released after 30 min or 120 min of the test respectively. The concentration of bosentan dissolved after 30 min from the solid dispersion high energy ball milled for 360 min was similar to that reported for quenched bosentan alone, but was much higher than that typical of high energy ball milled crude bosentan (98.63 ± 2.40 μg/mL). These findings indicate that the combination of bosentan and copovidone in equal parts (1:1) and their high energy ball milling, especially for 240 or 360 min, effectively enhanced bosentan release and could be used to form its supersaturated solutions in the gastrointestinal tract.

3.4.2. *Impact of copovidone load and processing method on bosentan release*

The concentration–time profiles presented in Figs. 10 and 11 show the relationship between the polymer load and the processing method on the release of bosentan in SGF and PBS of pH = 6.80 respectively. The impact of copovidone load was investigated on three levels, such as 20, 50 and 80 wt%. For the sake of comparison, the concentration–time profiles recorded for corresponding physical mixtures composed of the amorphous form of bosentan and copovidone, bosentan amorphous (ball milled alone), or crude bosentan in crystalline form were presented. They provided evidence that both processing methods enabled to obtain supersaturated systems where despite desupersaturation, the concentration of bosentan dissolved after 120 min was still higher than that typical of unprocessed formulations. This effect was the most pronounced for solid dispersions loaded with 50 or 80 wt% copovidone [NSD0.5 or NSD0.2] (Fig. 10 a, b). For high energy ball milled solid dispersion (milling time 240 min), the supersaturation level was similar i.e. 27.23 ± 2.82 μg/mL vs. 23.70 ± 1.16 μg/mL. However, the supersaturation was more stable when the solid dispersion was loaded with 80 wt% of copovidone (Fig. 10 a) than if 50 wt% of the polymer was used (Fig. 10 b). Interestingly, among all solid dispersions, the best performance showed nano spray dried sample NSD0.2, in which the polymer load prevailed (Fig. 10 a). In such a case, the supersaturation level was the highest, with the maximum at 31.17 ± 3.02 μg/mL reached after 45 min **(**Tab. A.3**)**. Importantly, only a slight reduction in supersaturation level was declared up to 90 min, which confirmed the stability of this supersaturated solution in SGF. Then, the concentration of bosentan decreased further, and after 120 min, it was almost the same as that typical of the corresponding high energy ball milled solid dispersion (BM0.2), that is, 23.64 ± 1.79 μg/mL. Both values were far higher than the equilibrium solubility of crude bosentan **(<2 μg/mL)** or even that of the physical mixture **(ca. 11 μg/mL)** loaded with amorphous bosentan **(**Tab. A.3**)**. This result could be related not only to the amorphization of bosentan and its dispersion within the hydrophilic matrix, but also to the reduction of the particle size of the hydrophobic drug up to the submicrometer range upon nano spray drying **(**Fig. 8**)**.

When the polymer load was the lowest, i.e. 20 wt% (BM0.8), the concentration time profile recorded for the ball milled solid dispersion was similar to that of the physical mixture composed of bosentan amorphous and copovidone with a maximum drug concentration around 11 μg/mL (Fig. 10 **c**, Tab. A.3). In such a case, desupersaturation started after 15 min of the test. Due to the recrystallization of the

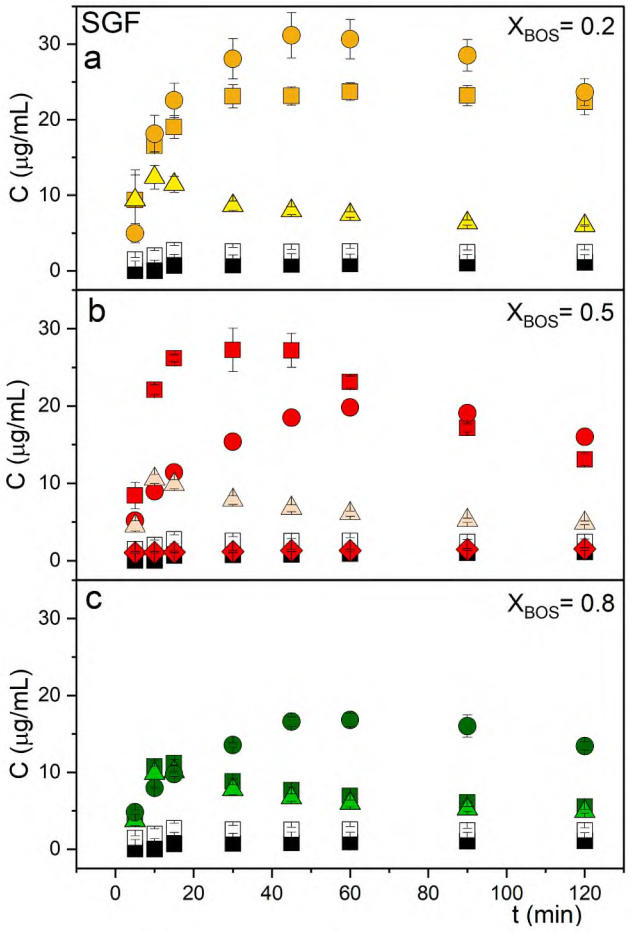

Fig. 10. Impact of the processing method on the concentration–time profiles recorded in SGF. The weight fraction of bosentan (X_{BOS}) in the binary formulation is: (a) 0.2 in yellow; (b) 0.5 in red; (c) **0.8** in green. Formulations ball milled for 240 min (solid squares), nano spray dried formulations (circles), physical mixtures of amorphous bosentan with copovidone (triangles), amorphous bosentan (open squares), crude bosentan **monohydrate** (black squares). (For interpretation of the references to colour in this figure legend, the reader is referred to the web version of this article.)

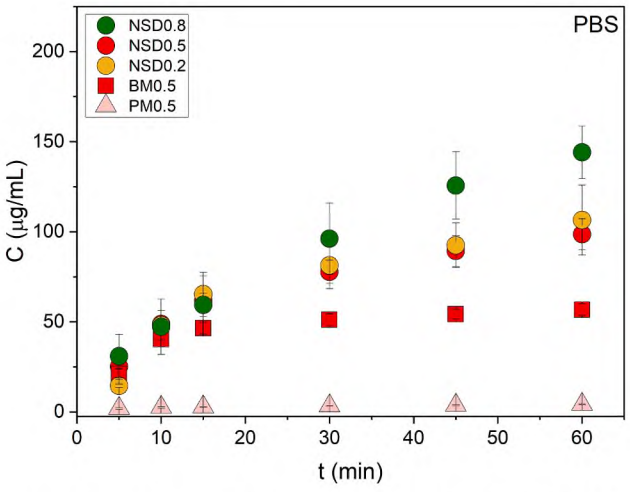

Fig. 11. Release of bosentan from ball milled (BM) and nano spray dried (NSD) solid dispersions in copovidone determined in PBS of pH = 6.80. Physical mixture **(1:1)** loaded with crystalline bosentan (PM0.5) was shown for comparison.

amorphous form, the concentration of the drug dissolved after 120 min was close to that of the crude bosentan. From the nano spray dried formulation (NSD0.8), bosentan gradually dissolved to finally reach the maximum of 16.82 ± 0.73 μg/mL after 60 min, then its concentration slowly lowered (Fig. 10 **c**, Tab. A.3).

Fig. 11 shows the concentration–time profiles of nano spray dried formulations determined in PBS with pH = 6.80. For the sake of comparison, the performance of ball milled amorphous solid dispersion (BM0.5) and crystalline physical mixture (PM0.5) was also shown. The relationship between the hydrophilic polymer load in nano spray dried solid dispersions and the supersaturation level differed from that described in SGF. Once the drug was highly ionized, polymer matrix formed diffusion layer whose thickness controlled its diffusion rate. After the initial burst release due to the rapid wetting of the hydrophobic bosentan by hydrophilic copovidone, the diffusion layer formed as much as the polymer dissolved, which controlled its further release. Thus, if the polymer load was high, the diffusion rate slowed and finally, the formulation loaded with the lowest amount of copovidone showed the highest supersaturation (144.04 ± 14.64 μg/mL). In addition, particle size played also an important role. The behavior of the ball milled solid dispersion (BM0.5) of higher particle size and irregular particle shape than the corresponding nano spray dried formulation was less favorable with much lower level of supersaturation (56.72 ± 3.27 μg/mL vs. 74.94 ± 6.60 μg/mL).

4. Conclusions

The results of this study provide evidence for the first time that the amorphous solid dispersion of bosentan can be formed using copovidone as a matrix-forming agent upon high-energy ball milling and nano spray drying. Three main factors were critical, i. e. the polymer load, the kind of coprocessing method, and the process parameters, because they determined the morphology of the final product and the bosentan release rate. The nano spray drying process ensured a unique opportunity to prepare submicrometer spherical particles loaded with bosentan and copovidone, while the particles of high energy ball milled formulations were larger than 20 μm. Moreover, their shape was irregular, and a wide particle size distribution resulted from the presence of agglomerates. It was shown that the combination of the drug amorphization and its particle size reduction enabled to reach high supersaturation levels, particularly when nano spray dried or high energy ball milled dispersions loaded with 80 wt% copovidone were studied in the gastric environment. Importantly, the coprocessing of bosentan with copovidone facilitated the amorphization of the drug and ensured the long-term stability of the amorphous form upon storage at ambient conditions. Analysis of concentration time profiles recorded in the intestinal milieu showed that the copovidone load may be crucial to control the release rate of bosentan. Among the amorphous formulations prepared by high energy ball milling, the best properties had these coprocessed for at least 240 min.

Finally, both high energy ball milling and nano spray drying can be considered as interesting technological approaches to prepare enabling formulations, especially when only a small amount of the compound is available.

Declaration of Competing Interest

The authors declare that they have no known competing financial interests or personal relationships that could have appeared to influence the work reported in this paper.

Acknowledgements

The research was carried out thanks to Sonata Bis grant no DEC-

2019/34/E/NZ7/00245 financed by the National Science Centre in Poland and *BGF-Séjour scientifique ed. 2020* grant funded by the French Embassy in Poland on behalf of the French Government.

Research data for this article.

Krupa, Anna; Strojewski, Dominik; Majda, Dorota; Wegrzyn, Agnieszka (2023), "Dataset related to amorphous solid dispersions composed of a poorly soluble drug - bosentan & copovidone", Mendeley Data, V1, doi: 10.17632/t8z4nhv2j7.1

Appendix A. Supplementary material

Supplementary data to this article can be found online at https://doi.org/10.1016/j.ejpb.2023.05.014.

References

[1] J. Dingemanse, P.L.M. van Giersbergen, Clinical pharmacology of bosentan, a dual endothelin receptor antagonist, Clin. Pharmacokinet. 43 (2004) 1089–1115.
[2] D.E. Kohan, J.G. Cleland, L.J. Rubin, D. Theodorescu, M. Barton, Clinical trials with endothelin receptor antagonists: What went wrong and where can we improve? Life Sci. 91 (2012) 528–539, https://doi.org/10.1016/j.lfs.2012.07.034.
[3] H.-J. Seyfarth, N. Favreau, C. Tennert, C. Ruffert, M. Halank, H. Wirtz, J. Mössner, J. Rosendahl, P. Kovacs, H. Wittenburg, Genetic susceptibility to hepatoxicity due to bosentan treatment in pulmonary hypertension, Ann. Hepatol. 13 (2014) 803–809, https://doi.org/10.1016/S1665-2681(19)30983-4.
[4] A. Minecka, K. Chmiel, K. Jurkiewicz, B. Hachuła, R. Łunio, D. Żakowiecki, K. Hyla, B. Milanowski, K. Koperwas, K. Kamiński, M. Paluch, E. Kamińska, Studies on the Vitrified and Cryomilled Bosentan, Mol. Pharm. 19 (2022) 80–90, https://doi.org/10.1021/acs.molpharmaceut.1c00613.
[5] A. Krupa, F. Danède, A. Węgrzyn, D. Majda, J.-F. Willart, Thinking of bosentan repurposing – A study on dehydration and amorphization, Int. J. Pharm. 622 (2022), 121846, https://doi.org/10.1016/j.ijpharm.2022.121846.
[6] H.-J. Lee, Y.-B. Kwon, J.-H. Kang, D.-W. Oh, E.-S. Park, Y.-S. Rhee, J.-Y. Kim, D.-H. Shin, D.-W. Kim, C.-W. Park, Inhaled bosentan microparticles for the treatment of monocrotaline-induced pulmonary arterial hypertension in rats, J. Control. Release. 329 (2021) 468–481, https://doi.org/10.1016/j.jconrel.2020.08.050.
[7] T. Panda, D. Das, L. Panigrahi, Formulation Development of Solid Dispersions of Bosentan using Gelucire 50/13 and Poloxamer 188, J. Appl. Pharm. Sci. 6 (2016) 027–033, https://doi.org/10.7324/JAPS.2016.60904.
[8] P.N. Kendre, P.D. Chaudhari, Effect of amphiphilic graft co-polymer-carrier on physical stability of bosentan nanocomposite: Assessment of solubility, dissolution and bioavailability, Eur. J. Pharm. Biopharm. 126 (2018) 177–186, https://doi.org/10.1016/j.ejpb.2017.06.024.
[9] P.N. Kendre, P.D. Chaudhari, S.P. Jain, S.K. Vibhute, An effort to augment solubility and efficiency of the oral bosentan-bucco-adhesive drug delivery system using graft co-polymer as the carrier, Polym. Bull. 78 (2021) 5851–5871, https://doi.org/10.1007/s00289-020-03412-z.
[10] A. Doty, J. Schroeder, K. Vang, M. Sommerville, M. Taylor, B. Flynn, D. Lechuga-Ballesteros, P. Mack, Drug Delivery from an Innovative LAMA/LABA Co-suspension Delivery Technology Fixed-Dose Combination MDI: Evidence of Consistency, Robustness, and Reliability, AAPS PharmSciTech. 19 (2018) 837–844, https://doi.org/10.1208/s12249-017-0891-1.
[11] K. Almansour, R. Ali, F. Alheibshy, T.J. Almutairi, R.F. Alshammari, N. Alhajj, C. Arpagaus, M.M.A. Elsayed, Particle Engineering by Nano Spray Drying: Optimization of Process Parameters with Hydroethanolic versus Aqueous Solutions, Pharmaceutics. 14 (2022) 800, https://doi.org/10.3390/pharmaceutics14040800.
[12] C. Arpagaus, PLA/PLGA nanoparticles prepared by nano spray drying, J. Pharm. Investig. 49 (2019) 405–426, https://doi.org/10.1007/s40005-019-00441-3.
[13] C. Arpagaus, Pharmaceutical Particle Engineering via Nano Spray Drying - Process Parameters and Application Examples on the Laboratory-Scale, Int. J. Med. Nano Res. 5 (2018) 1–15. https://doi.org/10.23937/2378-3664.1410026.
[14] C. Arpagaus, A. Collenberg, D. Rütti, E. Assadpour, S.M. Jafari, Nano spray drying for encapsulation of pharmaceuticals, Int. J. Pharm. 546 (2018) 194–214, https://doi.org/10.1016/j.ijpharm.2018.05.037.
[15] K. Cal, K. Sollohub, Spray Drying Technique. I: Hardware and Process Parameters, J. Pharm. Sci. 99 (2010) 575–586, https://doi.org/10.1002/jps.21886.
[16] K. Sollohub, K. Cal, Spray Drying Technique: II. Current Applications in Pharmaceutical Technology, J. Pharm. Sci. 99 (2010) 587–597, https://doi.org/10.1002/jps.21963.
[17] M. Mirankó, L. Trif, J. Tóth, T. Feczkó, Nanostructured micronized solid dispersion of crystalline-amorphous metronidazole embedded in amorphous polymer matrix prepared by nano spray drying, Adv. Powder Technol. 32 (2021) 2621–2633, https://doi.org/10.1016/j.apt.2021.05.037.
[18] M. Beck-Broichsitter, B. Strehlow, T. Kissel, Direct fractionation of spray-dried polymeric microparticles by inertial impaction, Powder Technol. 286 (2015) 311–317, https://doi.org/10.1016/j.powtec.2015.08.033.
[19] S. Kumar, J. Shen, B. Zolnik, N. Sadrieh, D.J. Burgess, Optimization and dissolution performance of spray-dried naproxen nano-crystals, Int. J. Pharm. 486 (2015) 159–166, https://doi.org/10.1016/J.IJPHARM.2015.03.047.
[20] P.F.M. Oliveira, J.-F. Willart, J. Siepmann, F. Siepmann, M. Descamps, Using milling to explore physical states: the amorphous and polymorphic forms of dexamethasone, Cryst. Growth Des. 18 (2018) 1748–1757, https://doi.org/10.1021/acs.cgd.7b01664.
[21] E. Elisei, J.-F. Willart, F. Danède, J. Siepmann, F. Siepmann, M. Descamps, Crystalline polymorphism emerging from a milling-induced amorphous form: the case of chlorhexidine dihydrochloride, J. Pharm. Sci. 107 (2018) 121–126, https://doi.org/10.1016/j.xphs.2017.07.003.
[22] F. Ngono, J.-F. Willart, G. Cuello, M. Jimenez-Ruiz, F. Affouard, Lactulose: a model system to investigate solid state amorphization induced by milling, J. Pharm. Sci. 108 (2019) 880–887, https://doi.org/10.1016/j.xphs.2018.09.013.
[23] A. Newman, S.M. Reutzel-Edens, G. Zografi, Coamorphous active pharmaceutical ingredient-small molecule mixtures: considerations in the choice of coformers for enhancing dissolution and oral bioavailability, J. Pharm. Sci. 107 (2018) 5–17, https://doi.org/10.1016/j.xphs.2017.09.024.
[24] S. Baghel, H. Cathcart, N.J. O'Reilly, Theoretical and experimental investigation of drug-polymer interaction and miscibility and its impact on drug supersaturation in aqueous medium, Eur. J. Pharm. Biopharm. 107 (2016) 16–31, https://doi.org/10.1016/j.ejpb.2016.06.024.
[25] A. Krupa, D. Majda, W. Mozgawa, J. Szlęk, R. Jachowicz, Physicochemical properties of bosentan and selected PDE-5 inhibitors in the design of drugs for rare diseases, AAPS PharmSciTech. 18 (2017) 1318–1331, https://doi.org/10.1208/s12249-016-0599-7.